A Comparison of GOES Moisture-Derived Product and GPS-IPW Data during IHOP-2002

DANIEL BIRKENHEUER AND SETH GUTMAN

NOAA/Forecast Systems Laboratory, Boulder, Colorado

(Manuscript received 14 October 2004, in final form 6 May 2005)

ABSTRACT

Geostationary Operational Environmental Satellite (GOES) sounder–derived total column water vapor is compared with other data sources obtained during the 2002 International H_2O Project (IHOP-2002) field experiment. Specifically, GPS-derived total integrated precipitable water (GPS-IPW) and radiosonde observations (raob) data are used to assess GOES bias and standard deviation. GPS integrated water calculated from signal delay closely matches raob data, both from special sondes launched for the IHOP-2002 exercise and routine National Weather Service (NWS) soundings. After examining the average differences between GPS and GOES product total precipitable water over the full diurnal cycle between 26 May and 15 June 2002, it was discovered that only 0000 UTC time differences were comparable to published comparisons. Differences at other times were larger and varied by a factor of 6, increasing from 0000 to 1800 UTC, and decreasing thereafter. Reasons for this behavior are explored to a limited degree but with no clear answers to explain the observations. It is concluded that a component of the GOES total precipitable water error (between sonde launches) might be missed when solely assessing the data against synoptic raobs.

1. Introduction

The International H_2O Project (IHOP-2002), a multiagency field experiment over the southern Great Plains of North America from 13 May to 25 June 2002, was undertaken to improve the characterization of water vapor variability in time and space and the understanding and prediction of convection. The primary focus of the Forecast Systems Laboratory (FSL) was to examine the ability to measure and analyze water vapor in several preconvective environments, including convective initiation, low-level jet scenarios, quantitative precipitation forecasting, and general model forecast comparisons. Many of these issues were discussed in a 2-day Water Vapor Intercomparison Workshop held in Boulder, Colorado, on 2–3 October 2003 (Parsons 2002).

As a part of this exercise, FSL teamed with the Office of Research and Applications (ORA) in the National Environmental Satellite, Data, and Information Service (NESDIS), and the Cooperative Institute for Meteorological Satellite Studies (CIMSS) at the University of Wisconsin—Madison to evaluate various Geostationary Operational Environmental Satellite (GOES) sounder products. The 3×3 pixel-averaged version of the three-layer experimental product (Schmit et al. 2002) has been used in FSL's LAPS analysis and model assimilation system for some time as an independent measure of water vapor (Birkenheuer 1999, 2001). The CIMSS 3×3 pixel-averaged product for the exercise was derived from nominal *GOES-8* data and is representative of conventional weather service products.

This note highlights the findings of the specially produced (but following the conventional algorithm) 3×3 pixel-averaged *GOES-8* total precipitable water (TPW) product data compared with integrated (total atmospheric column) precipitable water (IPW) vapor retrievals derived from GPS observations made at about 41 sites during IHOP-2002.

2. GOES product data for testing

The NESDIS/CIMSS three-layer precipitable water product integrates GOES sounding retrievals to provide a measurement of the layer and total precipitable water in clear and partly cloudy conditions (Schmit et al. 2002). The product provides moisture in three

Corresponding author address: Dr. Daniel Birkenheuer, NOAA/Forecast Systems Laboratory, Mail Code R/FS1, 325 Broadway, Boulder, CO 80305-3328.
E-mail: Daniel.L.Birkenheuer@noaa.gov

sigma-p layers plus a total column value. For this examination, only the TPW data were used for comparison to GPS-IPW data derived for local zenith. The GOES moisture product has been in existence for more than a decade. The GOES retrieval algorithm uses radiances from either a 5 × 5 or 3 × 3 set of averaged pixels to determine both representative radiance and cloud conditions essential for the retrieval processing. In this experiment, 3 × 3 pixel averages (~35 km × 46 km coverage for the IHOP-2002 area) were available from the experimental CIMSS *GOES-8* product.

The 3 × 3 pixel-averaged product dataset generated from *GOES-8* at CIMSS is ~2.5 times greater than the GPS sampled volume, but this is not considered a significant factor since GPS wet refractivity measurements are highly correlated (Wolfe and Gutman 2000). Furthermore, since microwave radiometer (MWR) and GPS water vapor are highly correlated, any comparison between GOES and MWR (Schmit et al. 2002) should also be valid for a GOES–GPS comparison. The CIMSS product used Eta model forecasts for its first guess, and model bias could influence the final GOES moisture product. The retrieval method acts on the a priori or first-guess profile derived from a forecast model and modifies it to match the radiance data in the retrieval processing.

The GOES data were available twice per hour to coincide with the Local Analysis and Prediction System (LAPS) 30-min cycles beginning at 20 and 50 min past each hour over both 12- and 4-km analysis domains. Each cycle represented the data available up to the prior 20-min time. More important for this study, however, was that the GOES data files contained a precise time for each computed moisture record in the file for a specific GOES scan. This true scan time was used when pairing the data with the GPS information.

3. GPS water vapor measurements

Integrated precipitable water vapor can be retrieved with arbitrary temporal resolution from tropospheric signal delays estimated by ground-based GPS receivers using the technique described in Bevis et al. (1992), Duan et al. (1996), and Fang and Bock (1998). The zenith tropospheric delay (ZTD) or the total excess signal delay caused by the constituents of the lower atmosphere, primarily the troposphere directly over the site, is defined as

$$\mathrm{ZTD} = \int n(s)\, ds, \tag{1}$$

where $n(s)$ is the index of refraction along the line-of-sight signal path from the GPS antenna to the satellite.

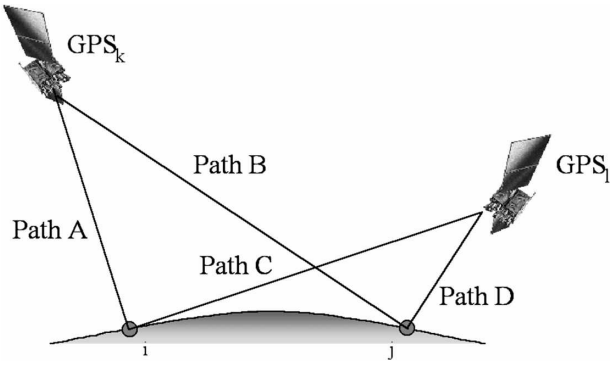

FIG. 1. A double difference (DD) is formed from ionospheric free carrier phase GPS observables derived from simultaneous observations of two satellites (k and l) by two GPS reference stations (i and j). DD = (path A − path B) − (path C − path D).

The tropospheric signal delay is estimated by first forming an "ionospheric free" carrier phase observation (Φ_{IF}) to eliminate the impact of the dispersive ionosphere,

$$\Phi_{\mathrm{IF}} = \Phi_{L1} - \frac{f_{L2}}{f_{L1}}\Phi_{L2}, \tag{2}$$

where f_{L1} = 1575.42 MHz, f_{L2} = 1227.60 MHz, and Φ denotes carrier phase. A "double difference" (DD) is then formed to remove receiver and satellite clock biases, as illustrated in Fig. 1.

The refractivity of the neutral (i.e., nondispersive) atmosphere is dominated by a dry (or hydrostatic) component caused by the total mass of the atmosphere, and a wet component caused by the dipole moments of the water vapor molecules along the paths of the GPS radio signals (Smith and Weintraub 1953):

$$N = 77.6\,\frac{P_d}{T} + 70.4\,\frac{P_v}{T} + 3.739\,\frac{P_v}{T^2}, \tag{3}$$

where N is total refractivity [$(n - 1) \times 10^6$], n is the index of refraction, P_d is atmospheric pressure (hPa), P_v is water vapor pressure (hPa), and T is temperature.

In terms of the relative contributions of the wet and dry refractivity terms to the total signal delay, the hydrostatic component contributes about 90%–95%, and the wet term contributes 5%–10% in exactly the same proportion as the wet and dry constituents of the free atmosphere. Because of the large time- and space-scale variability of the hydrostatic component, and its overwhelming contribution to the magnitude of the total delay (but not its variability, which is dominated by the variability of water vapor), we assume that the observed signal delay depends primarily on satellite elevation (α) above the horizon. The GPS signal delay along a single path to a satellite TD(α) is then modeled in

terms of an unknown "zenith-scaled tropospheric delay" (ZTD) and known elevation-angle-dependent mapping functions for the wet (M_W) and dry (M_D) delays, respectively (Niell 1996):

$$\mathrm{TD}(\alpha) = M_D(\alpha)\mathrm{ZTD} + M_W(\alpha)\mathrm{ZTD}. \quad (4)$$

Since there are currently 6–10 GPS satellites at different elevations in view at all times, solutions for the ZTD are overdetermined and are estimated with high accuracy as a nuisance parameter in either a relative or absolute sense. Duan et al. (1996) used a technique (Mikhail 1976) whereby ZTD is estimated in an absolute sense at each station in a network of continuously operating GPS reference stations, and this is the technique currently implemented at the National Oceanic and Atmospheric Administration (NOAA)/Forecast Systems Laboratory (FSL) (Wolfe and Gutman 2000) and used in this study.

In the process of scaling the GPS signal delays to the local zenith and averaging them (usually over a period of 30 min to reduce random measurement error), all information about the delays along an individual line –of sight (or slant path) are irretrievably lost. The resulting measurement is actually a weighted average of the signal delays within the field of view of the antenna: a radius of about 11 km at midlatitudes (Wolfe and Gutman 2000). These 30-min measurements, time stamped at the midpoint of the interval, have much in common with GOES TPW products or a radiosonde moisture sounding, since they all represent a volumetric average.

The separation of ZTD into its wet and dry components [Eq. (3)], and retrieval of integrated TPW from the water vapor mixing ratio (P_v/T) is carried out in a straightforward manner as follows.

1) Calculate the zenith-scaled hydrostatic or "dry" delay (ZHD) from an atmospheric pressure measurement made at the orthometric height of the GPS antenna using the Saastamoinen (1972) formulation.
2) Subtract ZHD from ZTD to derive the zenith-scaled wet delay (ZWD).
3) Map ZWD into TPW using a transfer function (Π) defined in Eq. (5):

$$\Pi = \frac{10^6}{\rho R_v \left[\frac{k_3}{T_m} + k_2'\right]}, \quad (5)$$

where R_v is specific gas constant for water vapor, k_3 and k_2' are gas constants at microwave frequencies (after Smith and Weintraub 1953), and T_m is water-vapor-weighted mean temperature of the atmosphere, where

$$T_m = \frac{\int \left(\frac{P_v}{T}\right) dz}{\int \left(\frac{P_v}{T^2}\right) dz}. \quad (6)$$

Several T_m estimation techniques have been proposed, including the use of atmospheric models (Bevis et al. 1994) and a best fit in space and time to global radiosonde measurements (Ross and Rosenfeld 1997). In this study, we used the coefficients derived from linear regression between a large number of surface and radiosonde observations (Bevis et al. 1992). The estimated error in Π using this approach is about 2%–4%. By examining Eq. (5), we conclude that the dominant source of water vapor retrieval error comes not from the wet delay mapping function but from errors in estimating ZTD as a free parameter in the solution of the double difference equation (Jensen et al. 2002). These errors, which are largely uncorrelated, include GPS satellite orbit and earth rotation parameters, mismodeling the phase centers of the GPS antennas, errors in calculating the position of the antenna at a site, and noise introduced by the site environment, primarily multipath.

Assessments of the accuracy of GPS-TPW retrievals come from comparisons with other moisture sensing systems in the United States and elsewhere. For the most part, NOAA studies have been carried out at the Department of Energy Southern Great Plains (SGP) Atmospheric Radiation Measurement (ARM) Cloud and Radiation Testbed (CART) Central Facility near Lamont, Oklahoma. As seen in Fig. 2, comparisons between GPS and radiosonde-derived PW at the ARM CART site between 1996 and 1999 reveal no long-term bias and a standard deviation of about 2 mm PW. Comparisons by other institutions at facilities around the world are fully consistent with these results (e.g., Basili et al. 2004; Haas et al. 2001; Emardson et al. 2000; Tregoning et al. 1998), and together they indicate that the accuracy of GPS-TPW retrievals is comparable to radiosonde measurements made under both operational and experimental conditions, including those encountered during IHOP-2002.

It should be noted that when making the comparisons between GPS-derived TPW and that measured by radiosondes, most of the above references also compared GPS-TPW with that measured using collocated passive zenith-pointing microwave water vapor radiometers (as did Revercomb et al. 2003 and Westwater et al. 1998). The results in all cases were comparable to the raob results: small average bias and comparable (but somewhat smaller) differences. The importance of this result is that, regardless of the observing systems

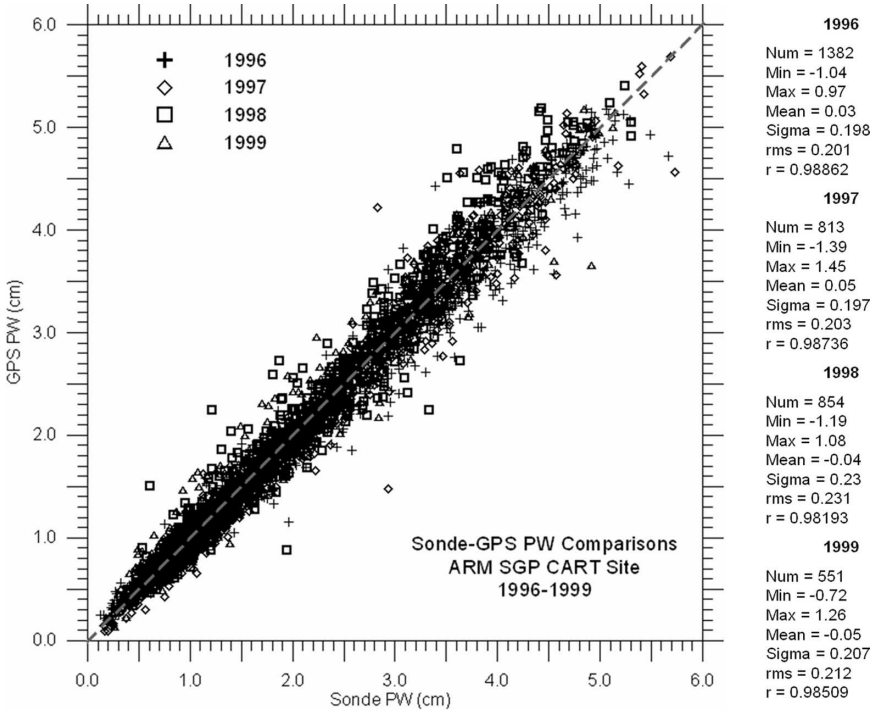

FIG. 2. Comparison of 3600 GPS-IPW retrievals and radiosonde PW over 3 yr at the ARM CART facilities near Lamont, OK.

being evaluated, the results are consistent, and conclusions based upon one set of comparisons are probably valid for another.

Figure 3 is a scatterplot that compares GPS and integrated radiosonde moisture observations at five closely spaced locations in the ARM SGP region during IHOP-2002. Four outliers (differences exceeding 2 sigma) were removed prior to computing the statistics. When the intercept is near zero and the slope of the regression is very close to 1.0, a very low bias should exist in the difference. Standard deviation of the differences appears to run under 0.15 cm. The best matches in data occur in the dry region of the plot, under 2.5 cm of IPW. As discussed previously, TPW comparisons between GPS and raob are similar to those between GPS and passive microwave water vapor radiometers (WVRs). The importance of this is that Schmit et al. (2002) showed that the averaged *GOES-8* TPW product is comparable to WVR-TPW, with bias differences on the order of 0.040-cm bias and standard error 0.180 cm. Even though radiosonde data are often considered the "gold standard" for the water vapor profile and integrated water, the error in raob data alone (Revercomb et al. 2003) may obscure the quality of the integrated measurement from the remote sensed data, such as GOES and GPS. This is the basis for our speculation that a GOES–GPS comparison might be superior to raob differences and may better portray comparative quality between the 3×3 derived product image (DPI) data. Even so, as will be shown later, we did examine comparisons to sonde data as part of this exercise, but

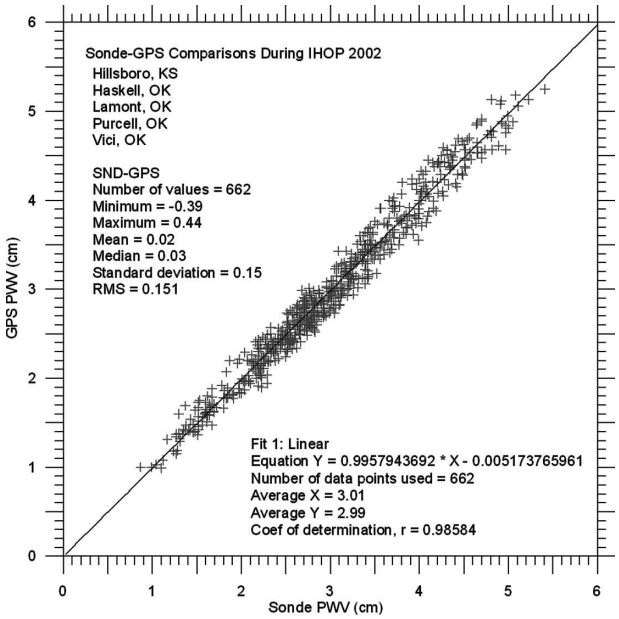

FIG. 3. A comparison of collocated raob and GPS-TPW measurements during IHOP-2002 with four outliers ($\Delta > 2\sigma$) removed.

it should be stressed that our main considerations were given to GOES–GPS differences. One thing that sonde data comparisons do illustrate is that the GPS data were performing perhaps just as well during IHOP-2002 against sonde data as they have in past studies.

4. Test operation

Error in the spatial collocation of the two datasets is also a consideration in this comparison study, from both the total accuracy and precision standpoints. The precision standpoint is far easier to estimate. The GPS data locations were known with very high accuracy, given that GPS propagation delay computations depend on knowing the GPS location to within a fraction of a centimeter. The GOES data records provided a location of the derived moisture from spacecraft navigation and were reported with a resolution of 0.001° in latitude and longitude. Thus, the GOES data had an inherent uncertainty on the order of ~0.15 km, orders of magnitude less than the grid spacing in the 12-km analysis, and more than an order of magnitude less than the 4-km grid spacing.

The accuracy of GOES data navigation (frame registration) is another matter. If imager navigation errors are any indication of sounder navigation accuracy, response to satellite maneuvers might cause errors in the specified latitude and longitude records to as much as 10 km (authors' experience). There was no attempt in this comparison to track such error; operational constraints on imager navigation/registration are assumed nominal at 95% of the time (Kelly et al. 1996) and are therefore not considered a large factor in this evaluation.

The comparison was set up using the GOES 3 × 3 and the corresponding GPS data. Time and space constraints were used to pair the data. First, a set of GPS and GOES differences was computed using the constraint of ≤24 min and ≤10 km separation. This resulted in a dataset of ~9000 pairs of the 3 × 3 data covering the extent of the exercise. Even if GPS and GOES were perfectly centered, the volumes of atmosphere measured were not identical. However, unlike point raob measurements, both sources were volumetric measures and more alike in that sense.

5. Results

Comparison results are shown in Fig. 4, a scatterplot that contrasts the *GOES-8* product with GPS. The short, line segment is a least squares linear fit. The scatterplot trend shows a moist bias in GOES-TPW growing with increasing TPW. The cause of this pattern

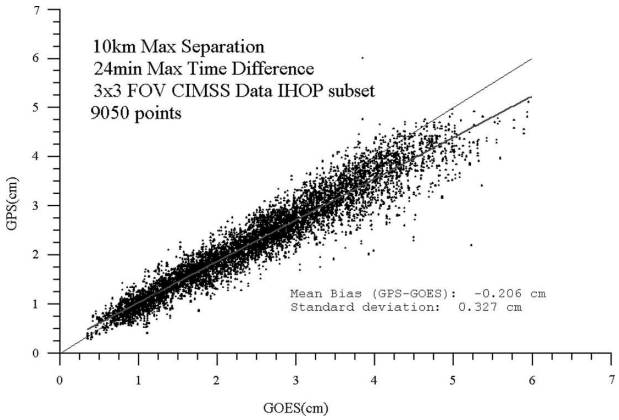

FIG. 4. A comparison of GPS and *GOES-8* 3 × 3 CIMSS pixel-averaged DPI data with GPS IHOP-2002 measurements. Mean difference was −0.206 cm (GPS − GOES) and a sigma of 0.327 cm. The sample set was 9050 points.

is unclear, or at least not evident from this data comparison. Also, there appears to be a widening of the overall scatter as moisture increases. This might be expected since at very low (near zero) TPW, all systems seem to have less of a problem describing that extreme, possibly also due to airmass characteristics. It is possible that a dry air mass contains more homogeneous TPW values, whereas higher TPW regions may have more variability in the horizontal moisture distribution. This is only speculation, and we are hopeful that this kind of question will be answered by additional research in the IHOP-2002 reanalysis and close scrutiny of in situ moisture measured with other independent high-resolution sensors.

A tabulated collection of data statistics from different measurements contrasting this comparison with other published studies is shown in Table 1. It is interesting to note that the mean difference between the GPS and CIMSS 3 × 3 pixel-averaged data during IHOP-2002 was less than that shown by Wolfe and Gutman (2000); however, the standard deviation was greater. The GOES 3 × 3 rmsd values are similar to other published comparisons.

6. Hourly breakdown of moisture

After inspection of the TPW scatterplots and their abnormally high bias (when compared to other published values), it was decided to make an hourly assessment of the CIMSS 3 × 3 GOES–GPS differences. This revealed an intriguing result: Fig. 5 shows that the differences are lowest at 0000 UTC and then increase with another minor minima in difference near 1200 UTC. In addition, the greatest rmsd values are seen near

TABLE 1. Comparison of instrument differences from this study and others. The first column shows the different instruments used in the mean difference computation in the second column. Column 3 is the standard deviation of the differences, and column 4 is rmsd computed as the square root of the sum of column 2 squared with column 3 squared. The last column lists the number of data points used in each computation.

Instruments compared	Difference (cm)	Std dev diff (cm)	Rmsd (cm)	Points studied
GPS–*GOES-8* 3 × 3 CIMSS (IHOP-2002)	−0.206	0.327	0.39	9050
GPS–GOES*	−0.23	0.23	0.33	560
GOES-8–sonde**	−0.069	0.346	0.35	6568
GPS–sonde*	−0.049	0.20	0.21	64
GPS–sonde (IHOP-2002)	−0.02	0.15	0.15	662

* Wolfe and Gutman (2000).
** Schmit et al. (2002).

0900 UTC (primarily due to scatter) and then at 1700 UTC (mainly due to bias).

The computed bias (relative to GPS) at 0000 UTC was very close to the "reported" error characteristics for the GOES data (Schmit et al. 2002) where raob surface pressures were used to define the base of the integrated column. Various ideas have been offered to explain this, but none of them really resolves this curious hourly behavior. It is probably not valid to assume that synoptic times are favored, since they might include raob data. Due to latency, the model first guess was not likely influenced by the synoptic raob data until sometime after 0000 or 1200 UTC. One could also consider the effect of the retrieval background, in this case the National Centers for Environmental Prediction (NCEP) Eta Model forecast might have a bias. Research shows that the Eta Model has a suspected moist bias in situations where the model is slow to advance dry air intrusions (Massie and Rose 1997).

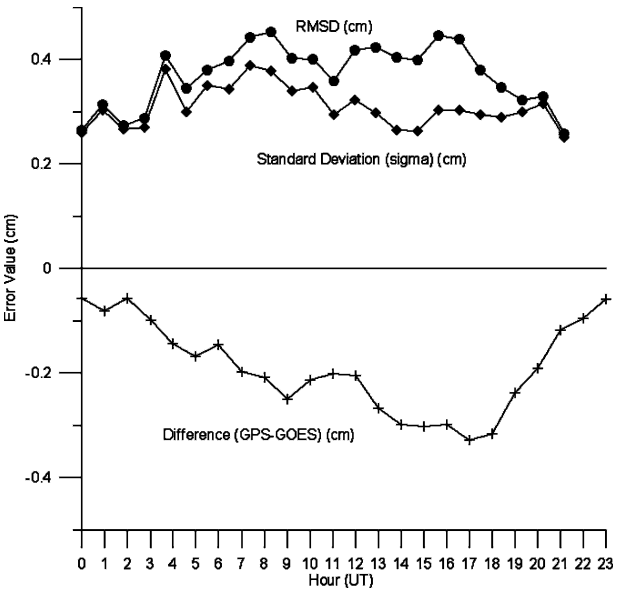

FIG. 5. Hourly error characteristics of the GOES–GPS comparison. The statistic studied is the same as shown in Figs. 4–6. The perceived positive bias in GOES measurements occurs when the difference (GPS − GOES) is negative. Sigma is plotted in the positive domain, as is rmsd, defined in Table 1.

Clouds might play a part in the hourly bias trends as well. Perhaps the 0000 UTC satellite images were more cloud-free than early morning times, since there may have been a lot of nocturnal storm cloud residue over the region in the early morning that finally dissipated in the early afternoon. It is known that fractional cloudiness can cause problems with the GOES retrieval algorithm, since the IR radiances are strongly influenced by clouds and the retrieval algorithm is tailored for clear-sky conditions. During the day, the visible band is used to detect clouds via a threshold method, which might partially explain differences between day and night results. The cloud scenario is possible, but, at the time of writing, this has not yet been fully investigated.

We investigated the effect of retrieval surface pressure error. If the surface pressure in the GOES retrieval were too high, this would cause the integration calculation to use more surface moisture than it should have otherwise. Thus, this might lead to a positive moist bias in GOES.

The role of pressure measurements in ground-based GPS meteorology is to objectively parse the zenith tropospheric signal delay into its wet and dry components. As described by Duan et al. (1996), the zenith tropospheric delay is estimated as a free parameter in the measurement of the antenna position. The delay is assumed to have only a hydrostatic and a wet component: the former is caused by the mass of the atmosphere and the latter by the dipole moments of the water vapor molecules in the atmosphere above the GPS antenna. As discussed previously, the hydrostatic component is derived from a surface pressure measurement (Saastamoinen 1972) with little error (Resch 1984). A 1-hPa surface pressure measurement error maps into a dry refractivity error equivalent to a GPS-TPW retrieval error of approximately 0.03 cm.

Surface pressure data measurements made at all GPS

sites in the IHOP-2002 domain are made with recently calibrated digital barometers. In addition, the accuracy of the surface pressure measurements, which are constantly monitored using the technique described by Miller and Fozzard (1994), indicate that the maximum differences between the observations and the Mesoscale Analysis and Prediction System (MAPS) and the Rapid Update Cycle (RUC) Surface Assimilation System (MSAS/RSAS) never exceeded 1.0 hPa. In contrast, the pressures from the GOES integration were obtained from the GOES data records and supplied from the integrated retrieval profile. The ultimate source of the surface pressure in the GOES processing was the background model (Eta) used for the profile first guess that is derived from analyzed surface pressure observations.

Similar to the moisture data, Fig. 6 shows a surface pressure scatterplot with the same criteria as in Fig. 4. Data points are within 10-km and 24-min space and time separation. These data were then examined on an hourly basis to construct the plot in Fig. 7, which is similar to Fig. 5 and shows the rmsd, sigma, and bias of surface pressures. There appears to be a negative pressure GOES bias at the low-pressure end of the plot and a possible positive pressure GOES bias near 925 hPa.

The hourly pressure bias in Fig. 7 is seen to be very low (overall) with extremes at 0800 and 2000 UTC with a magnitude of about ±2 hPa. The hourly bias and rmsd data in Fig. 7 show little or no correlation with the moisture error in Fig. 5. The pressure bias is small enough in Fig. 7 that the light gray sigma line is lost in the plotted rmsd line for most hours, since most of the contribution to rmsd is from sigma (scatter). Furthermore, a surface bias pressure of 2 hPa will only affect the integrated PW profile computation on the order of 0.01 cm, about an order of magnitude too small to contribute to the observed differences in the moisture plot. Therefore, pressure differences were ruled out as a possible explanation for the discrepancies plotted in Fig. 5.

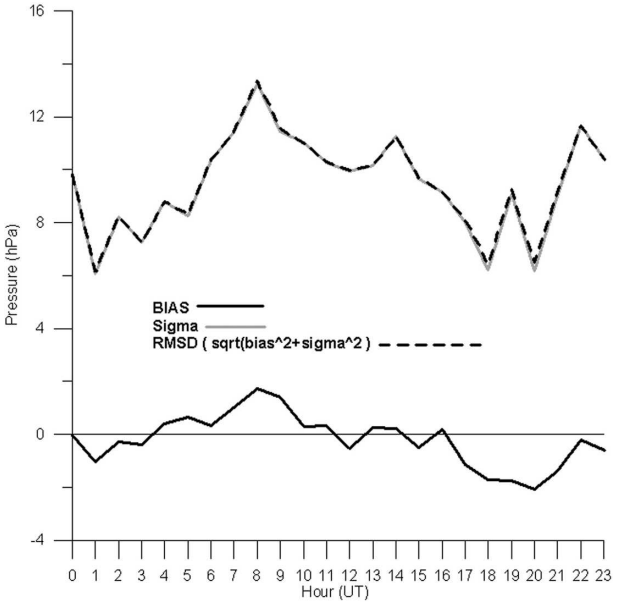

FIG. 7. The hourly breakdown of the pressure data from Fig. 6 summarized by statistics of bias, sigma, and rmsd.

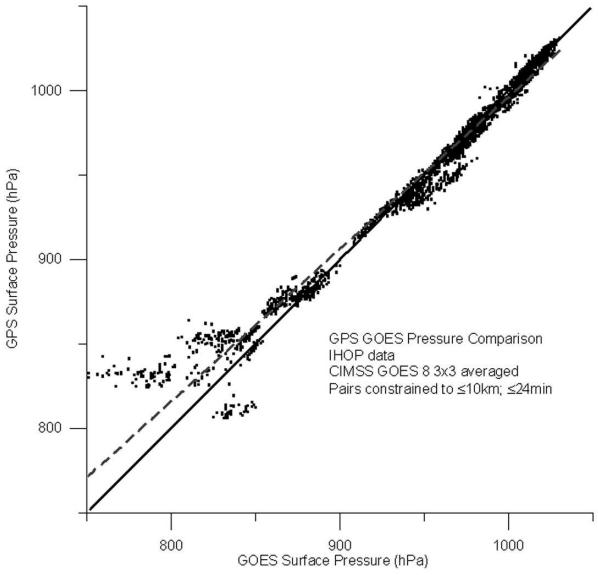

FIG. 6. Scatterplot showing the GPS vs GOES surface pressures during the IHOP-2002 experiment. The dashed line is a least squares fit to the data.

7. Summary

Several interesting features were noted in this study. Wolfe and Gutman (2000) cite GPS–GOES average differences of 0.23 cm, similar to the differences shown here for the CIMSS averaged data. In all GPS–GOES scatterplots, better agreement is shown at lower water vapor levels; in other words, the scatter broadens with greater moisture amounts. This same effect is evident in Schmit et al. (2002), which shows a comparison of the GOES DPI products with ground-based microwave radiometer data.

The nature of the hourly trend of GOES bias is curious, and there are no current clear-cut reasons for this behavior. The 0000 UTC error values agree closely with published values. Asynoptic error values were found to be higher than anticipated or indicated by published values. This indicates that synoptic error measures may not be truly representative of the GOES product error.

More study is needed to explain the hourly rmsd and bias observations at asynoptic times.

Acknowledgments. We would like to acknowledge the contributions of Susan Sahm, Kirk Holub (FSL), Jaime Daniels, and Gary Gray (NESDIS).

REFERENCES

Basili, P., S. Bonafoni, V. Mattioli, P. Ciotti, and N. Pierdicca, 2004: Mapping the atmospheric water vapor by integrating microwave radiometer and GPS measurements. *IEEE Trans. Geosci. Remote Sens.,* **42,** 1657–1665.

Bevis, M., S. Businger, T. A. Herring, C. Rocken, R. A. Anthes, and R. H. Ware, 1992: GPS meteorology: Remote sensing of atmospheric water vapor using the global positioning system. *J. Geophys. Res.,* **97,** 15 787–15 801.

——, ——, S. Chiswell, T. A. Herring, R. A. Anthes, C. Rocken, and R. H. Ware, 1994: GPS meteorology: Mapping zenith wet delays onto precipitable water. *J. Appl. Meteor.,* **33,** 379–386.

Birkenheuer, D., 1999: The effect of using digital satellite imagery in the LAPS moisture analysis. *Wea. Forecasting,* **14,** 782–788.

——, 2001: Utilizing variational methods to incorporate a variety of satellite data in the LAPS moisture analysis. Preprints, *11th Conf. on Satellite Meteorology and Oceanography,* Madison, WI, Amer. Meteor. Soc., 273–276.

Duan, J. M., and Coauthors, 1996: Remote sensing atmospheric water vapor using the global positioning system. *J. Appl. Meteor.,* **35,** 830–838.

Emardson, T. R., J. Johansson, and G. Elgered, 2000: The systematic behaviour of water vapor estimates using four years of GPS observations. *IEEE Trans. Geosci. Remote Sens.,* **38,** 324–329.

Fang, P., and Y. Bock, 1998: A sliding-window procedure for super near realtime continuous GPS water vapor estimation using predicted orbits. *Ann. Geophys.,* **16** (Suppl.), C379.

Haas, J., H. Vedel, M. Ge, and E. Calais, 2001: Radiosonde and GPS zenith tropospheric delay (ZTD) variability in the Mediterranean. *Phys. Chem. Earth,* **26A,** 6–8.

Jensen, A. B. O., C. C. Tscherning, and F. Madsen, 2002: Integrating numerical weather predictions in GPS positioning. *Proc. ENC GNSS-2002 Conf.,* Copenhagen, Denmark, ESA, 8 pp.

Kelly, K. A., J. F. Hudson, and N. Pinkine, 1996: GOES 8/9 image navigation and registration operations. *Proc. SPIE,* **2812,** 777–788.

Massie, D. R., and M. A. Rose, 1997: Predicting daily maximum temperatures using linear regression and ETA geopotential thickness forecasts. *Wea. Forecasting,* **12,** 799–807.

Mikhail, E. M., 1976: *Observations and Lease Squares.* IEP, 497 pp.

Miller, P. A., and R. L. Fozzard, 1994: Real-time quality control monitoring of hourly surface observations at NOAA's Forecast Systems Laboratory. Preprints, *10th Conf. on Numerical Weather Prediction*, Portland, OR, Amer. Meteor. Soc., 7–9.

Niell, A. E., 1996: Global mapping functions for the atmospheric delay at radio wavelengths. *J. Geophys. Res.,* **101,** 3227–3246.

Parsons, D., cited 2002: IHOP_2002 Water Vapor Intercomparisons Workshop Presentations. [Available online at http://www.atd.ucar.edu/dir_off/projects/2002/IHOPwsOct03/presentations.html.]

Resch, G. M., 1984: *Effects of Electromagnetic Wave Propagation through the Atmosphere*. Springer-Verlag, 213 pp.

Revercomb, H. E., and Coauthors, 2003: The ARM program's water vapor intensive observation periods. *Bull. Amer. Meteor. Soc.,* **84,** 217–236.

Ross, R., and S. Rosenfeld, 1997: Estimating mean weighted temperature of the atmosphere for Global Positioning System applications. *J. Geophys. Res.,* **102,** 21 719–21 730.

Saastamoinen, J., 1972: Introduction to practical computation of astronomical refraction. *Bull. Geod.,* **106,** 383–397.

Schmit, T. J., W. F. Feltz, W. P. Menzel, J. Jung, A. P. Noel, J. N. Heil, J. P. Nelson, and G. S. Wade, 2002: Validation and use of GOES sounder moisture information. *Wea. Forecasting*, **17,** 139–154.

Smith, E. K., and S. Weintraub, 1953: The constants in the equation for atmospheric refractive index at radio frequencies. *Proc. IRE,* **41,** 1035–1037.

Tregoning, P., R. Boers, D. O'Brien, and M. Hendy, 1998: Accuracy of absolute precipitable water vapor estimates from GPS observations. *J. Geophys. Res.,* **103,** 28 701–28 710.

Westwater, E. R., Y. Han, S. I. Gutman, and D. E. Wolfe, 1998: Remote sensing of total precipitable water vapor by microwave radiometers and GPS during the 1997 water vapor intensive operating period. *Proc. IGARSS'98*, Seattle, WA, IEEE Geoscience and Remote Sensing Society and Cosponsors, 2158–2162.

Wolfe, D. E., and S. I. Gutman, 2000: Developing an operational, surface-based, GPS, water vapor observing system for NOAA: Network design and results. *J. Atmos. Oceanic Technol.,* **17,** 426–440.